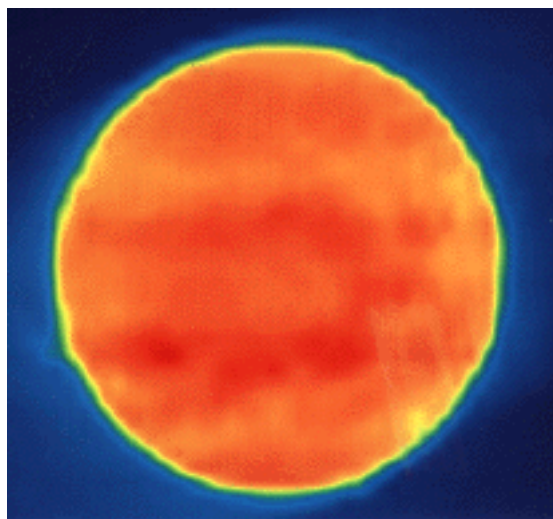


Technical

Radio Observations of Two Solar Eclipses

It doesn't take an array of expensive equipment to make your own radio telescope. Here's how one radio amateur monitored solar radio emission during two solar eclipses.

**By Darrel Emerson, AA7FV/G3SYS
3555 E Thimble Peak
Tucson, AZ 85718
e-mail: demerson@heineken.tuc.nrao.edu**



An image of the Sun at a wavelength of 3 mm, observed with the NRAO 12-meter Telescope at Kitt Peak, Arizona, on July 12, 1991. On the previous day, there had been a solar prominence visible on the western (right) limb of the sun, but this has now disappeared. On the eastern limb a new prominence has appeared. The structure within the solar disk is much more stable, and is very similar to that observed the previous day. The data were observed by D. T. Emerson and P. R. Jewell. The National Radio Astronomy Observatory (NRAO) is operated under cooperative agreement with the NSF.

In July 1991, a partial solar eclipse was visible from my location in Tucson, Arizona. The sun had been quite active that month, and solar noise had been easily detectable on 146 MHz with my rather poor OSCAR-13 satellite system. I thought it might be fun to see how the received solar emission varied during the eclipse. The results were, to me, a little surprising—more than fulfilling my hopes for an interesting experiment.

In May 1994, another partial solar eclipse was visible from my location. This time, I was able to record data at both 146 MHz and 436 MHz, again using my much-worse-than-average amateur-satellite receiving system. The July 1991 eclipse had been near the maximum of the sunspot cycle, but in May 1994, the sunspot number

was more characteristic of the approaching sunspot minimum. The results obtained this time were in complete contrast to the 1991 event, and just as interesting.

No Fancy Gear Needed

The equipment I use is very simple. Anyone with a VHF or UHF beam antenna and an AM or SSB receiver can monitor solar radiation. Apart from being very interesting in its own right, drastic changes in solar activity usually warn of similar changes in terrestrial radio propagation. During daylight hours, you can record your own solar data, and be much more up to the minute than the reports broadcast on WWV. The sun also makes a very useful radio source in the sky for checking out antennas and receivers; however, its strength at radio wavelengths—especially at meter-wavelengths—can vary by more than an order of magnitude. I found that being able to hear strong solar noise is no guarantee that the antenna and receiver system is working at good efficiency.

Observing the Sun

Figure 1 shows the main elements of the receiving setup, which is essentially identical at 146 and 436 MHz. I use a 10-element Yagi on 146 MHz and a 15-element Yagi on 436 MHz. Low-noise preamplifiers are used on both bands. The 436-MHz preamp is mounted at the antenna; the 146-MHz preamp is in the shack. My receiver is a Yaesu FTV-107 trans-verter feeding my aging Yaesu FT-102 transceiver. This I set to USB mode using a 2.8-kHz IF filter, with the AGC turned off and the RF and AF gains adjusted manually to ensure that all the receiver stages are operating linearly. The receiver audio output is taken from the radio's speaker jack, detected and smoothed by the circuit shown in Figure 2,¹ then recorded on my old Heath chart recorder. The audio transformer increases the audio noise voltage applied to the diode detectors; if the level is adequate, then the smoothed dc output voltage from this circuit is proportional to the RMS audio-output voltage of the receiver. The total receiver noise power is proportional to the square of this voltage. The same audio output is also fed to a simple analog-to-digital converter (ADC or A/D converter) driven by a personal computer, which samples the audio signal directly at a rate of a few kilohertz. For every second, the computer calculates the average of the RMS value of the several thousand samples of audio signal, and records this average together with the time of day. Together, the ADC and computer RMS calculation make an extremely linear power meter. This real-time preprocessing reduces the amount of raw data that needs to be stored on the computer's hard disk to manageable proportions, while still allowing later data editing of small samples of the data for interference, if necessary.

The listening frequencies were chosen to avoid—as much as possible—man-made interference, such as the harmonics from TV sets, computer time-base oscillators and satellite beacons. At my location, good frequencies are around 145.8 MHz and 435.6 MHz. I made no attempt to track the sun. Instead, I pointed the antennas (in azimuth and elevation) at the predicted position of the sun at the MIDQ2-point of the eclipse, and the sun drifts through the antenna pattern. Because the antennas have beamwidths of 30 or 40°, it took—depending on its precise elevation angle—more than three hours for the sun to move between the antenna's half-power points. The total duration of each eclipse was somewhat less than this, so in practice, the sun was easily visible to this receiving setup for significantly more than the duration of each eclipse.

The July 1991 Eclipse

For the 1991 observations, only 146-MHz data were recorded, using just the chart recorder, as the sun drifted through the antenna pattern. Several hours of data before and after the eclipse were obtained as well. The chart record was later digitized by hand (over a several-day period!) for further processing with a computer.

Figure 3 shows the receiver noise power sampled over a six-hour period. The times of the start, maximum and end of the eclipse are marked by vertical dashed lines. At maximum obscuration, 71% of the area of the sun's disc was covered by the moon. The relative sensitivity of the antenna in the direction of the sun is shown with a smooth dashed line; the signal peaks up slowly as the sun drifts into the antenna pattern. The sharp peaks in the data show the strong bursts of radio emission from the sun, characteristic at this wavelength of fairly high solar activity. The maximum peaks were some 10 times stronger than the background receiver noise level. From the known antenna and receiver parameters, the peak signal received at 146 MHz amounts to about 135 solar flux units (see Appendix A); this is about what is expected from a typical noise storm at this frequency.² There was no radio evidence of any effect of the solar eclipse until 1822 UTC, *58 minutes after the start of the eclipse*. At that point, all detectable solar emission disappeared within the space of about nine minutes. The emission did not start to reappear until 72 minutes later, at 1943 UTC, and was fully restored by 1951 UTC, *13 minutes before the end of the eclipse*, which occurred at 2004 UTC.

The fact that the radio emission disappeared and reappeared fairly abruptly partway through the eclipse indicates that most of the radio emission was occurring from *one discrete point* on the sun's surface, rather than from the entire solar disc. At the time the signal disappeared, the source of emission had to be located somewhere along the moon's leading edge over the solar disc. Similarly, at the time the emission reappeared, the source had to be located somewhere along the trailing edge of the moon's disc. If the outline of the moon is drawn over an image of the sun at the precise times of disappearance and reappearance of the signal, the intersection of these two outlines pinpoints the emission source. (Actually there are *two points* of intersection, but fortunately, only one of these is also inside the sun's disc.) Figure 4 illustrates this. From the precise time of disappearance and reappearance of the signal, this region could be located fairly accurately at 0.085° south and 0.131° east of the sun's center. Liberal use of the PC astrometric program *MICA*⁸ computed the solar and lunar sizes and precise coordinates as seen from my location during the eclipse.

The signals did not disappear and reappear quite instantaneously. From the rate of disappearance and reappearance, the extent of the emission region can be calculated; with some simple geometrical assumptions, the size comes out to be 0.06°. From this, the effective radio brightness temperature of the radiating region at 146 MHz can be calculated (see Appendix B). At the peaks of the sharp bursts seen in Figure 3, this is about 1 billion degrees!

From these simple observations, using an antenna with a beamwidth of approximately 40°, I've been able to locate a source of emission to better than *one hundredth of a degree*, and to measure the angular size of an emission region little more than *one twentieth of a degree* in extent! Of course, the precision has nothing to do with the antenna beamwidth, but depends on accurately knowing the correct time.

The May 1994 Eclipse

Another solar eclipse was visible in Tucson on May 10, 1994. Less than 100 miles south of Tucson, it was a perfect annular eclipse; I know, because I drove south to see it with my own (protected) eyes, leaving my radio equipment to operate and record data without me. From my home location, a maximum of 86% of the sun's disc was covered by the moon. On this occasion, data were recorded simultaneously by the computer at 146 MHz and 436 MHz, with the chart recorder also recording 146-MHz data as a backup. It's a long wait for the next eclipse, if the (unattended) computer crashes and there's no back-up recording at all! The sun was very quiet at this time. At 146 MHz, the peak solar intensity was much less than the receiver noise. In 1991, it had peaked 10 times greater than the background noise. The 146-MHz data were also marred by man-made interference. All in all, the sun was barely detectable with any certainty at this frequency.

The 436-MHz data were much better. The system noise at 436 MHz is lower than that at 146 MHz, and there was little or no man-made interference that day. The sun, however, was still relatively quiet. The peak antenna temperature due to the sun was still less than the background system noise. Changes in receiver noise detected when the sun drifted through the antenna's pattern were comparable to changes in background noise due to the galactic background structure as it also drifted through the pattern. Adding in receiver and other drifts over the approximately six hours of observations, at first sight, the 436-MHz data did not look too promising, either.

To try to sort out the solar radiation from other changes in background noise, I made an identical set of observations the day after this eclipse, keeping the antenna pointed in the same fixed direction. By comparing the eclipse observations with those of the following day, I hoped to identify what had really changed when the moon had drifted in front of the sun. This procedure would only work if the solar emission was fairly constant and about the same strength on both days—which turned out to be the case.

Figure 5 shows the ratio of the signals received on the two days: eclipse data of May 10 divided by the reference data of May 11. For each day, the one-second samples initially recorded were averaged into five-minute averages of the receiver noise power. This averaging considerably reduces the random fluctuations visible in the data. A small correction was also made for a slight but steady drift in receiver gain over the six-hour period. The result, shown in Figure 5, is an absolutely classic eclipse curve, just as can be found in optical astronomy textbooks. For comparison, below the measured data shown in Figure 5 is a theoretical eclipse curve calculated from the fraction of the solar disc that was covered by the moon throughout this eclipse. Again, liberal use was made of *MICA* to calculate this eclipse curve for my location. The good agreement between measurement and theory is quite remarkable. Unlike the July 1991 eclipse observed at 146 MHz, there were no significant discrete noise sources on the solar surface detected at 436 MHz on May 10 or May 11.

Having established how well the measurements agree with the simple theory, there are nevertheless some subtle differences. The measured curve is a little less sharp than the model at the minimum of emission, corresponding to the point of maximum obscuration. This is consistent with the solar emission at 436 MHz being either very slightly more extended than the optical disc, or being slightly peaked toward the center of the disc. The model has assumed a solar disc of uniform radio brightness, equal in extent to the optical disc.

The surface temperature at the center of the quiet sun at 436 MHz is about 300,000 K (see Note 2²). If the emission at 436 MHz is assumed to come from a uniform disc the same as the optical solar disc, then from the known properties of my antenna and receiver, my measurements imply a disc temperature of 275,000 K (see Appendix C). Considering all the uncertainties, this measurement is in almost surprising agreement with the established value.

These simple measurements have enabled a good measurement of the size of the radio sun at 436 MHz, and of the radio brightness of the disc. At least approaching the solar minimum, at 436 MHz, the solar corona cannot be a significant source of radiation. All this from a 30° antenna pattern!

The Sunspot Cycle

The 1991 observations were made at a time when the sun was quite active, close to the peak of the current 11-year sunspot cycle (Cycle 22). At the cycle peak, in July 1989, the smoothed sunspot number, *R*, was 158.1. The sunspot number of July 11, 1991 was 142, only a little below the 1989 peak. In May 1994, the situation is more representative of sunspot minimum; the sunspot number on May 10 was only 27. This is shown very clearly in Figure 6, which plots the monthly mean and the smoothed sunspot numbers from January 1989 to August 1994.⁴ The actual sunspot values for the cycle maximum in July 1989, and for the days of the eclipse in July 1991

and May 1994, are marked; these one-day points lie very close to the smoothed data values.

Although the 1991 and 1994 data presented here are of different frequencies, the results are typical of the difference between sunspot maximum and sunspot minimum. In 1991, near maximum, the solar emission was dominated by a tremendously strong, rapidly fluctuating discrete region. In 1994, approaching minimum, the eclipse curve shows there was very little emission from any discrete region, but a fairly uniform brightness over the entire solar disc.

Summary

Very simple equipment has been used to make some relatively precise measurements about the state of the sun during these solar eclipses. With or without an eclipse to provide the fun, anyone with a small VHF or UHF beam and a simple receiver (but not FM), can monitor the solar emission. Apart from being interesting in its own right, when combined with the WWV broadcasts, the extra up-to-date information on solar activity can only help in radio propagation predictions. It's another, fascinating facet to the hobby of Amateur Radio. Making and trying to calibrate these solar-eclipse observations really brought home to me quite how enormously variable the radio sun is, on time scales from less than one second—to decades.

Appendices

APPENDIX A

Calculation of Peak Solar Flux Received at 146 MHz

Given the antenna temperature of the source and knowing the gain of the antenna, the received solar flux can be calculated. The formulas used in this and the following appendixes can all be found in two books written by John Kraus, W8JK. [*Radio Astronomy* (New York: McGraw-Hill), 1966 and *Antennas* (New York: McGraw-Hill), 1988.]

At 146 MHz, the gain of my antenna is believed to be 14.2 dBi, or $G = 26$. The system noise at this frequency and in the direction of the sun at the time of the 1991 eclipse (but not including solar radiation) is estimated at 425 K; most of this is due to galactic background radiation. The capture area, A , of an antenna at wavelength λ is given by:

$$A = \frac{G_s}{4\pi} \lambda^2 \quad (\text{Eq 1})$$

This gives $A = 8.7 \text{ m}^2$.

The received flux density, S , for a source giving an antenna temperature, T , in units of $\text{W/m}^2\text{-Hz}$ is given by:

$$S = \frac{2kT}{A} \quad (\text{Eq 2})$$

where k is Boltzmann's constant (1.38×10^{-23} Joule/K). The factor 2 assumes equal power in both polarizations of the received radiation. The solar bursts received at 146 MHz in July 1991 were approximately 10 times stronger than the background receiver noise of 425 K. Using Eq 2, this gives a received solar flux density in these bursts of 135 solar flux units (sfu), where $1 \text{ sfu} = 10^{-22} \text{ W/m}^2\text{-Hz}$. This is the same unit as used for announcements of 2.7-GHz solar flux levels on WWV (at 18 minutes past each hour) and WWVH (at 45 minutes

past each hour). The referent of Note 1¹ specifies a “typical noise storm” at 100 MHz as 100 sfu, so my measurements correspond to a solar noise storm that was slightly stronger than average. The biggest uncertainty in this measurement is in the assumed antenna gain and system noise; the calculated peak flux density is probably accurate within about 20%

APPENDIX B

Calculation of Radio Brightness Temperature of the Hotspot

From the timing of the rate of disappearance and reappearance of the source of strong solar emission, it was estimated to have an angular extent of 0.06°. For a known flux density, S, the equivalent radio brightness temperature of that small region can be estimated using:

$$T = \frac{S^2}{2k\omega} \quad (\text{Eq 3})$$

where ω is the area of the emitting region measured in steradians. Using $S = 135$ sfu (Appendix A), this gives a radio brightness temperature of 2.7×10^9 K—well over one billion degrees! The biggest uncertainty here is probably in the assumed geometry of the hotspot necessary in deriving ω .

APPENDIX C

Calculating the Mean Solar-Disc Temperature at 436 MHz

At 436 MHz, the total receiver system noise (not including solar radiation) is estimated at 120 K, and the antenna gain is believed to be 16.5 dBi. (The receiver noise is only a small fraction of this 120 K; the rest comes mainly from ground radiation into the side lobes of the antenna, with some contribution from the galactic background.) Measuring the fractional depth of the minimum of the data shown in Figure 5, the change in antenna temperature as the moon partially obscured the sun can be found. Only 86% of the sun was covered, so the total additional antenna temperature expected from an uneclipsed sun can be derived; it is 65 K. Using Eq 1 in Appendix A, the capture area, A, of the antenna is 1.69 m². Using Eq 2 in Appendix A, the total flux measured from the sun at 436 MHz is calculated as 11 sfu. Using Eq 3 of Appendix B, with ω as the total area of the sun on May 10 1994, calculated by *MICA*, the mean apparent temperature at 436 MHz of the solar disc comes out to 275,000 K. From Allen's *Astrophysical Quantities* (Note 2²), the established temperature of the quiet sun at this frequency is 300,000 K. This falls well within the estimated error of my measurements.

Darrel Emerson was first licensed in 1964 as G3SYS and still holds that call. In addition to a BA in natural science from the University of Oxford, Darrel has a PhD in radio astronomy from the University of Cambridge, England. For a number of years, Darrel operated in Germany as DJ0OE and in France as F6HYR before moving to Arizona and picking up his AA7FV call. Currently, Darrel is employed by the National Radio Astronomy Observatory in Tucson, Arizona, working primarily with the 12-meter millimeter-wave radio telescope at Kitt Peak. Most of Darrel's Amateur Radio activity is on CW, but he spends a great deal of time listening for very weak signals with ridiculously inadequate equipment.

Notes

- (1) PC boards are available from FAR Circuits, 18N640 Field Ct, Dundee, IL 60118-9269. Price: \$3.50, plus \$1.50 shipping. A PC-board template is available from the Technical Department Secretary. Please send a business-size envelope with one First-Class stamp with your request for the EMERSON CHART

a business-size envelope with one First-Class stamp with your request for the EMERSON CHART RECORDER INTERFACE PC-BOARD.

- (2) Clabon Allen, *Astrophysical Quantities* (New York: Oxford University Press, Inc), 1964, p 188.
- (3) *MICA* (Multiyear Interactive Computer Almanac) is a program produced by the US Naval Observatory. *MICA* is available for PC/MS-DOS-compatible and Macintosh systems. Price: \$55 plus \$6 handling for either system. PC/MS-DOS version order no. PB93500163 (9 diskettes); Mac version order no. PB93500155 (4 diskettes). (A catalog of NTIS items—over 2 million—is available free of charge.—Ed) Please direct orders or inquiries concerning availability and pricing to: US Department of Commerce, NTIS, 5285 Port Royal Rd, Springfield, VA 22161, tel 703-487-4650; fax 703-321-8547.
- (4) *Solar Terrestrial Forecast and Review* “Recent Solar Indices (Preliminary) of the Observed Monthly Mean Values,” updated October 6, 1994, released by Solar Terrestrial Dispatch, PO Box 357, Stirling, Alberta, Canada, tel 403-756-2386, fax 403-756-3008. *The Solar Terrestrial Forecast and Review* (STFR) is a weekly electronic publication. The “Recent Solar Indices (Preliminary) of the Observed Monthly Mean Values” is an insert in the STFR that was originally compiled by the Space Environment Services Center and updated by the STD. This information is continually updated.

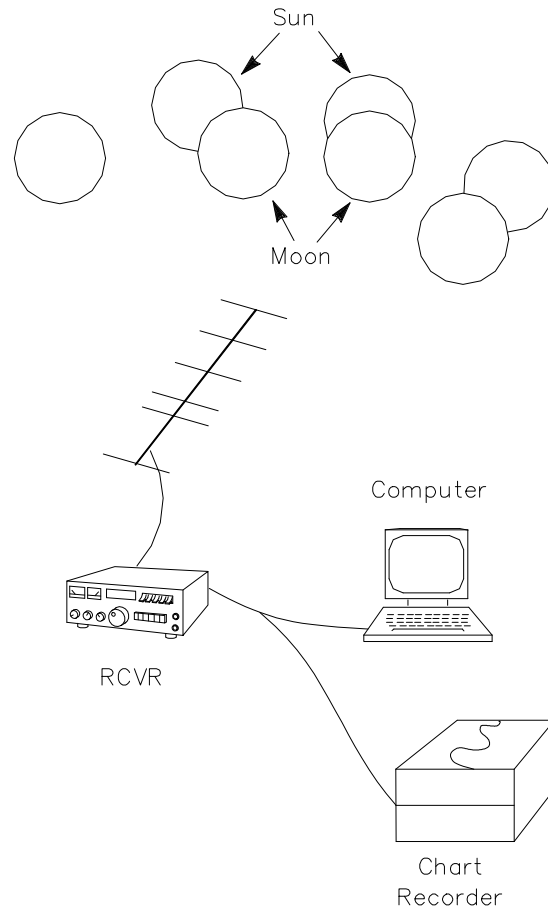


Figure 1—The simple radio telescope used for these observations. Although only one receiving setup is shown for simplicity, I use a 10-element Yagi on 146 MHz and a 15-element Yagi on 436 MHz. Low-noise preamplifiers

are used on both bands. The 436-MHz preamp is mounted at the antenna; the 146-MHz preamp is in the shack. I use a Yaesu FTV-107 transverter feeding a Yaesu FT-102 transceiver. Each antenna is pointed in a fixed direction—at the calculated position of the sun at the maximum of the eclipse. The receiver, tuned to 145.8 MHz or 435.6 MHz, detects the signal. The total power received is averaged over 1-second intervals and recorded on a chart recorder or digitized and sent to the computer.

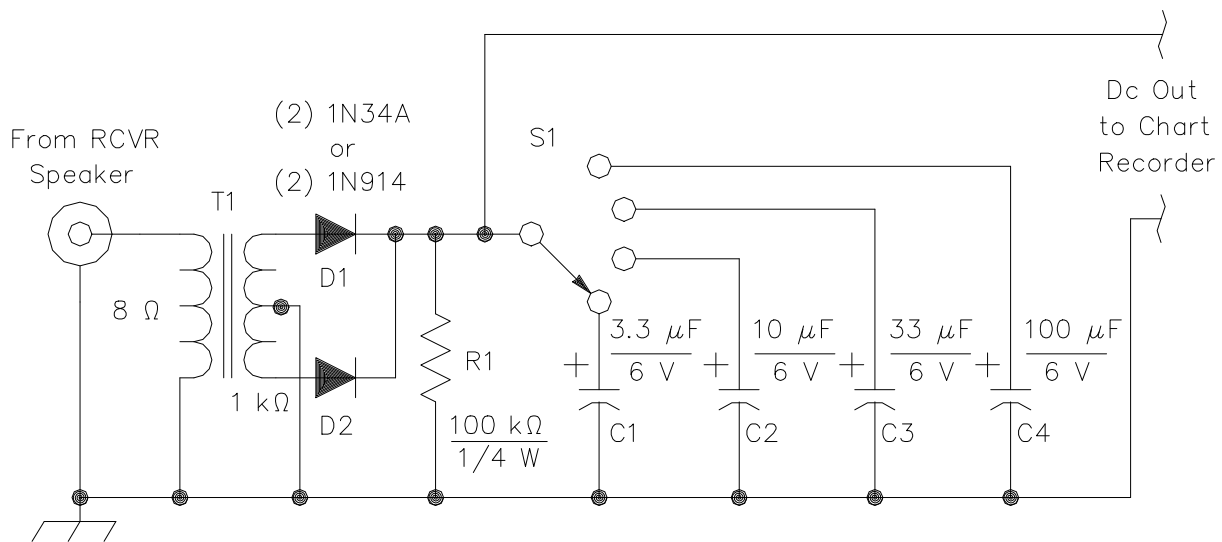


Figure 2—A simple interface used between the receiver's audio (speaker) output and the chart recorder. S1 selects a smoothing (integration) time of 0.3, 1, 3 or 10 seconds. Part values are not critical and equivalent parts can be substituted. Part numbers in parentheses are Radio Shack. The capacitor voltage ratings can be greater than 6 V.

C1—3.3 μF , 6 V (can be made by connecting in parallel a 1- μF [RS 272-1434] and 2.2- μF [RS 272-1435] tantalum capacitor).

C2—10 μF , 6 V (RS 272-1025)

C3—33 μF , 6 V (can be made by connecting in parallel a 10- μF [RS 272-1025] and 22- μF [RS 272-1026] electrolytic capacitor).

C4—100 μF , 6 V (RS 272-1028)

D1, D2—1N34A germanium diode (RS 276-1123)

R1—100 k Ω , 1/4 or 1/8 W (RS 271-1347)

S1—Single-pole, 4-position switch (RS 275-1385), 8 positions unused.

T1—Audio step-up transformer, with a center-tapped secondary. The transformer turns ratio is not critical. (You can use an RS 273-1380 audio-output transformer with the primary and secondary windings transposed.—Ed.)

Misc: PC board (see Note 1¹) or perf board, enclosure, input and output connectors, knob.

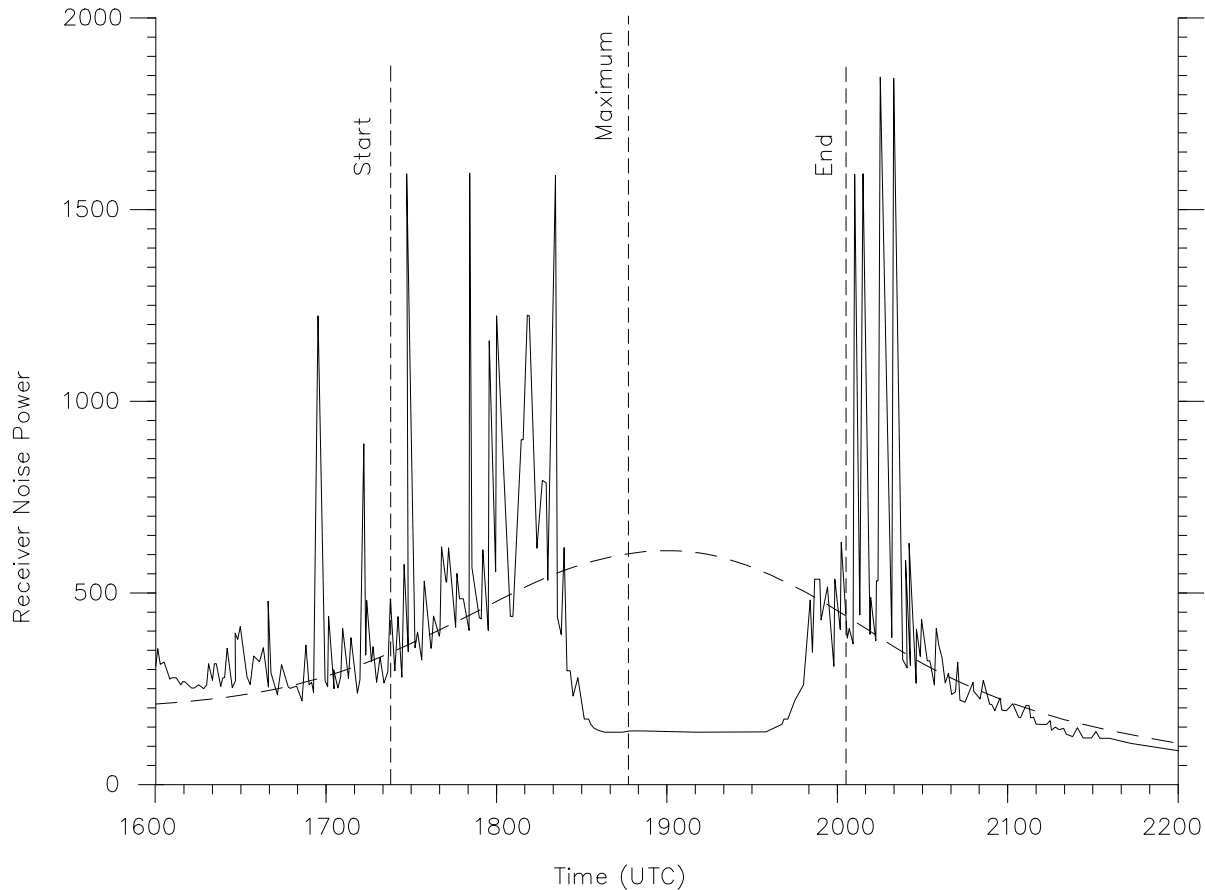
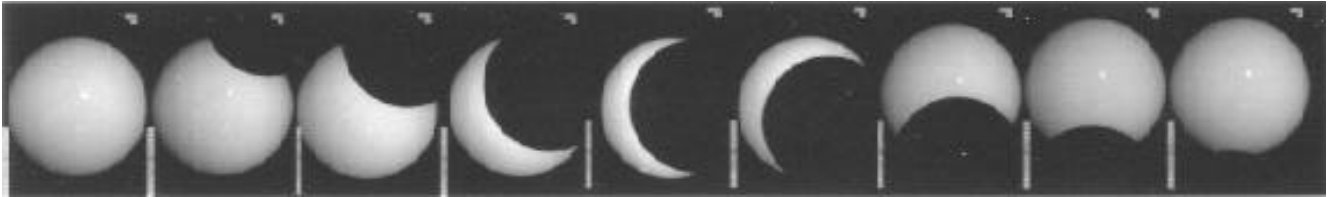


Figure 3—The signal received at 145.8 MHz over a six-hour period including the solar eclipse of July 11, 1991. The vertical axis is in arbitrary RMS units of receiver noise power. The intensity of the noise bursts gradually increases as the sun drifts into the antenna pattern. The start, maximum and end of the eclipse are marked by the three vertical dashed lines. The smoothly varying, curved dashed line indicates the expected variation in sensitivity due to the antenna response. The background level, due to a combination of galactic background noise and receiver noise, has not been subtracted from the data. The peak intensities of the solar noise bursts are approximately 10 times more powerful than the background receiver noise.



A collection of nine eclipse images (arranged in a vertical sequence) taken by the Big Bear Solar Observatory on May 10, 1994. These images were taken through a filter sensitive to light from the calcium K line (Ca II K). The images show the gradual progression of the moon moving in front of the sun over a period of about three hours. This image was combined from data provided courtesy of the Big Bear Solar Observatory via the Solar Terrestrial Dispatch.

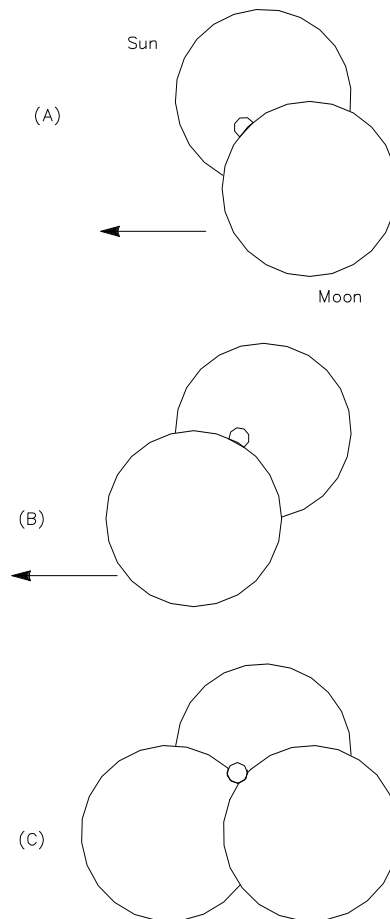


Figure 4—The position of the moon on the sun's disc at the time of disappearance, and of reappearance, of the strong emission detected at 146 MHz. The point of intersection of the lunar limbs defines precisely the position of the origin of the radiation. At A, the moon—moving to the left across the sun—is just beginning to obscure the radiating region. At B, the moon at a later time—still moving to the left—is beginning to uncover the radiating

region again. At C, by knowing the positions of the moon when the radiating zone is covered and then uncovered, the precise position of the active region on the sun can be found. This is at the inter-section of the respective leading and trailing limbs of the moon.

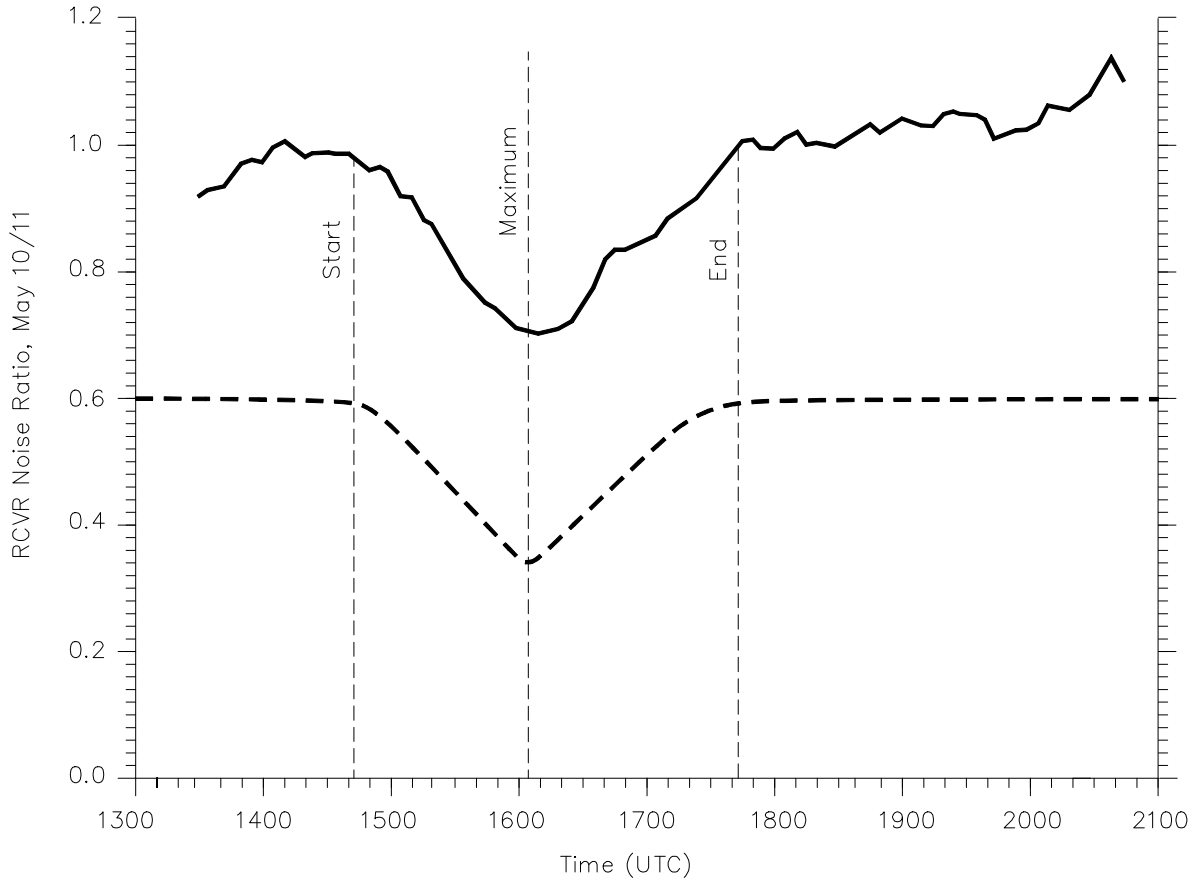
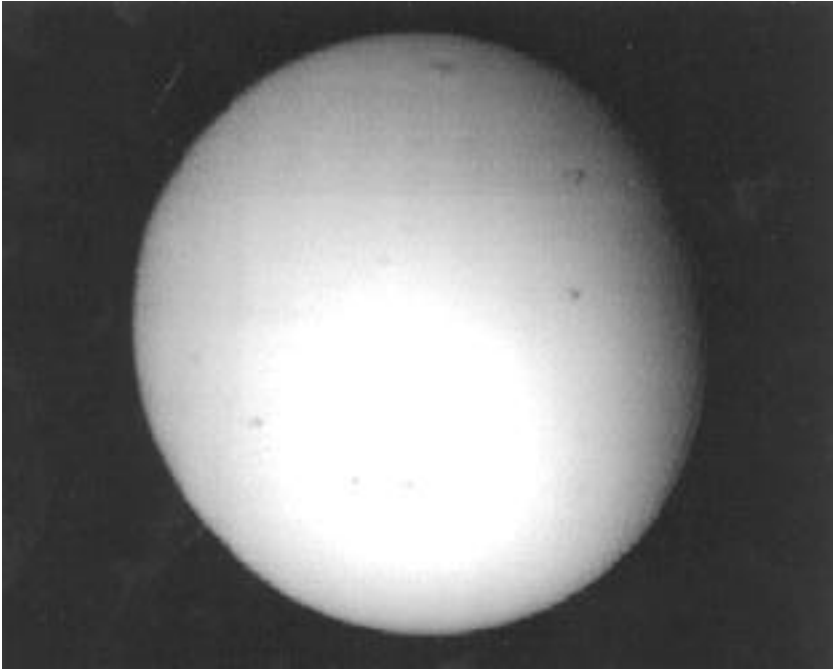
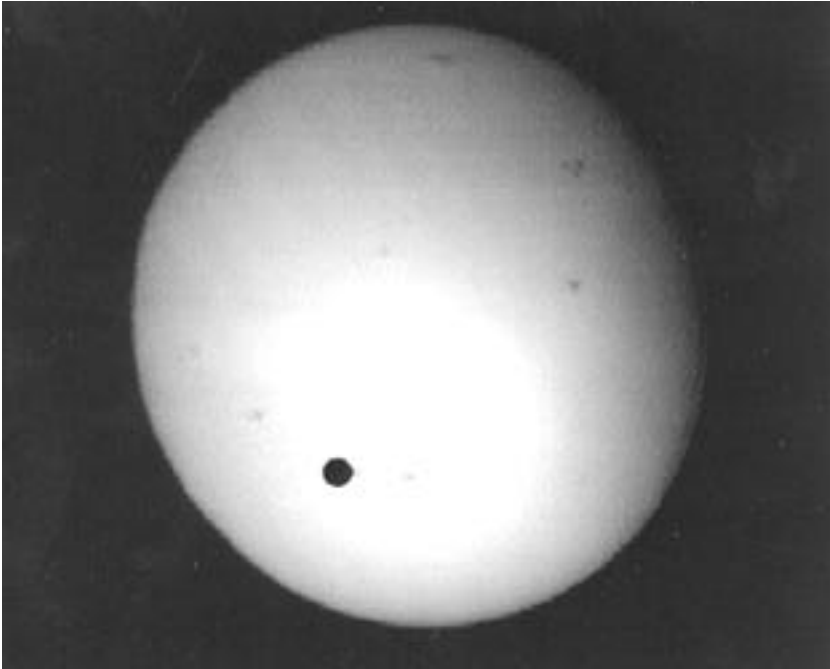


Figure 5—The upper curve shows the signal received at 435.6 MHz over a period of nearly eight hours on May 10, 1994, depicting the decrease in intensity during the solar eclipse. The lower, smooth, dashed line shows the shape of the eclipse curve expected for a solar disc of uniform radio brightness, equal in extent to the optical emission. As in Figure 3, the start, maximum and end times of the eclipse are marked by vertical dashed lines. The data of May 10 have been normalized by identical measurements made the following day, to remove variations due to galactic background emission drifting through the antenna pattern. The background receiver noise has not been subtracted from the data.



A white-light optical image recorded by Tom Folkers in Tucson, Arizona, at 1720 UTC on July 11, 1991, a few minutes before the start of the solar eclipse. The image was digitized from an RCA vidicon camera attached to an 80-mm Celestron telescope through a Thousand Oaks solar filter. Many sunspot regions can be seen, characteristic of an active Sun.



The same white-light image from Tom Folkers, showing many sunspot regions just before the July 1991 eclipse. A large black spot has been added to the image to show the position and approximate extent of the source of intense radio emission from the sun recorded at 146 MHz during this eclipse. Although the 146-MHz emission is close to one of the sunspot regions, it is significantly displaced from it.

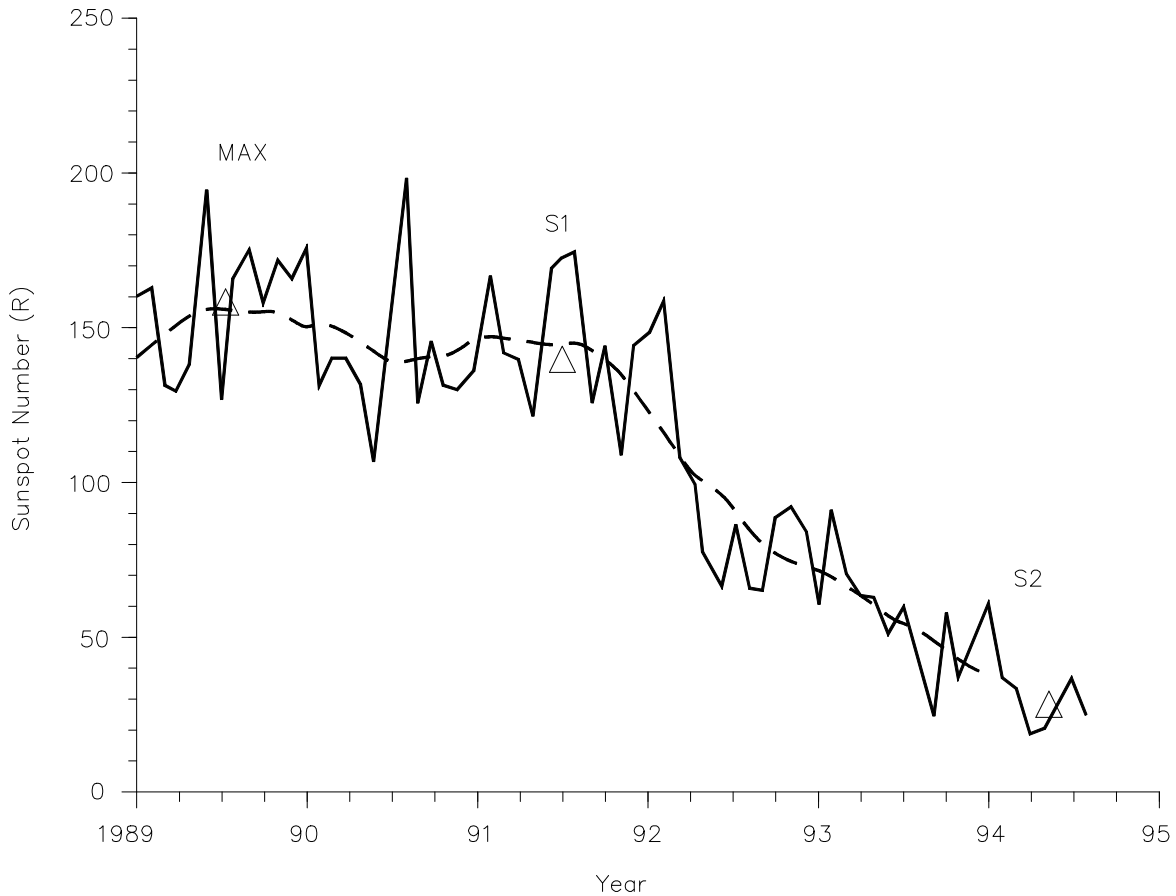


Figure 6—The monthly mean sunspot number, R, and the smoothed sunspot number, plotted from January 1989 through August 1994 (see Note 4⁴). The position of the peak of Cycle 22 in July, 1989 is marked MAX, with the sunspot numbers at the times of the 1991 and 1994 eclipses marked S1 and S2. In July 1991, the solar activity was almost as high as at the peak of 1989, but fell quite sharply between 1991 and the time of the May 1994 eclipse. The 1991 observations are characteristic of sunspot maximum, and the 1994 observations of sunspot minimum.

Is this Ewe for You?

Here's a really simple receiving antenna for 80 and 160-meter DXing.

**By Floyd Koontz, WA2WVL
6842 Wheeler Rd
Bloomfield, NY 14469**

As we approach the bottom of the sunspot cycle, MF and HF signals are weak and ambient noise is high. What every serious DX operator needs to improve signal-to-noise ratio is a directive receive antenna. In a